



Analysis of computerized tomography characteristics in gastrointestinal subepithelial lesions diagnosed through endoscopy or endovascular ultrasound

Gulsum Kilickap

Bilkent City Hospital, Department of Radiology, Ankara, Türkiye

ARTICLE INFO

Keywords:

Subepithelial lesions
Computerized tomography
Endoscopic ultrasonography

Received: May 22, 2024

Accepted: Jul 19, 2024

Available Online: 26.07.2024

DOI:

[10.5455/annalsmedres.2024.05.097](https://doi.org/10.5455/annalsmedres.2024.05.097)

Abstract

Aim: Subepithelial lesions (SEL) of the gastrointestinal tract are lesions arising from the mucosa, submucosa or muscularis propria. This study is aimed to assess diagnostic characteristics of SELs on computerized tomography (CT) and to present the localization, size, CT attenuation and contrast enhancement patterns of the lesions that may aid in making correct diagnosis.

Materials and Methods: Between December 2022 and March 2024, patients with a preliminary diagnosis of SEL on endoscopy or EUS and who underwent abdominal CT were retrospectively screened from the hospital database. Localization, size, pre-contrast and post-contrast Hounsfield Unit (HU) values of the lesions, and pathologic diagnoses were recorded and compared in patients with SEL.

Results: Pathologic diagnosis was available in 25 (23.4%) patients with SEL detected on CT. Among these, the most common lesion was gastrointestinal stromal tumors (GIST, 52%). In 22 (20.6%) patients, the lesion was not detected on CT. The lesions that could not be seen on CT were less than 2 cm in size. Gastrointestinal distension was insufficient in the majority of patients in whom the lesion could not be visualized on CT. While the HU values increased by approximately 3 times in patients diagnosed with neuroendocrine tumors (median [interquartile ranges] 36.5 [32 – 40] vs. 101.5 [81.5 – 127.5]; $p = 0.068$), the increase was approximately 2 times in those with GIST (30 [29 – 38] vs. 70 [57 – 77]; $p=0.003$).

Conclusion: This study presents several CT characteristics and pitfalls that may aid correct diagnosis of SELs with CT. SELs smaller than 2 cm in size and located in cardia are more likely to be missed with CT. Adequate gastric distention is crucial in correct diagnosis.



Copyright © 2024 The author(s) - Available online at www.annalsmedres.org. This is an Open Access article distributed under the terms of Creative Commons Attribution-NonCommercial-NoDerivatives 4.0 International License.

Introduction

Subepithelial lesions (SEL) of the gastrointestinal tract are lesions arising from the mucosa, submucosa, or muscularis propria and covered by the normal epithelium. They are usually detected incidentally during endoscopy and are most commonly located in the stomach. They may be neoplastic or non-neoplastic [1, 2]. It has been reported that 15% of these lesions are malignant at the time of diagnosis [3]. They are rarely symptomatic; however, large or ulcerated lesions may cause pain, bleeding, and obstruction [4, 5].

Subepithelial lesions may be due to intramural or extramural reasons. Extramural lesions develop due to compression of surrounding organs or lesions.

Endoscopic Ultrasonography (EUS) is the preferred method for diagnosis. The wall layer from which the lesion originates, size, echogenicity, contour, and the presence of vascularization with Doppler can be evaluated with EUS. EUS is superior to cross-sectional imaging methods, especially in showing from which wall layer the lesion originates [6, 7].

Computed Tomography (CT) allows evaluation of the relationship of the lesion with surrounding organs. Measuring the density of the lesions, detecting the presence of lymph nodes, and evaluating the relationship of the lesion with surrounding organs are the superior aspects of CT [8, 9]. However, it is difficult to differentiate the wall layer from which the lesion originates with CT [10, 11]. CT features may provide insight into the benign-malignant differentiation of the lesion. The large size of the lesion, heterogeneous contrast enhancement, irregular contour, and the

*Corresponding author:

Email address: gkilickap@yahoo.com.tr Gulsum Kilickap

presence of lymph nodes are findings that may suggest malignancy. In this study, we aimed to assess the diagnostic characteristics of endoscopy, EUS, and CT for diagnosing SELs, and to present the localization, size, CT attenuation, and contrast enhancement patterns of the lesions that may aid in making correct diagnosis in patients who underwent CT scan with a preliminary diagnosis of SEL on endoscopy or EUS.

Materials and Methods

Between December 2022 and March 2024, patients with a preliminary diagnosis of SEL on endoscopy or EUS and who underwent abdominal CT were retrospectively screened from the hospital data processing system. The keywords of subepithelial lesion, submucosal lesion, and SEL were screened on our database. Patients who underwent non-contrast abdominal CT and those who did not have preoperative CT were excluded (n=3) (Figure 1). CT images of the patients included in the study were evaluated by a radiologist with 15 years of experience in abdominal radiology. Localization, size, pre-contrast, and post-contrast Hounsfield Unit (HU) values of the SELs and the pathologic diagnoses were recorded.

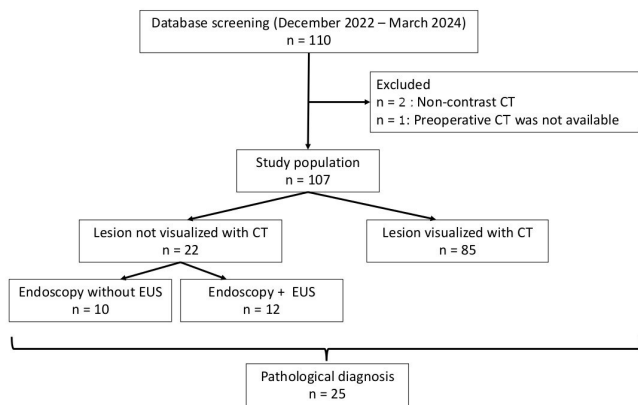


Figure 1. Flowchart for the study population.

This study was approved by the institutional ethics committee (Ankara Bilkent City Hospital Medical Research Scientific and Ethical Evaluation Board No. 2 (TABED), 15 May 2024; 2-24-165). As the study was made on the images that have been recorded on the hospital databases, informed consent was waived.

CT method

All of the patients underwent a 128-slice CT scan (GE Medical Systems, Milwaukee, WI, USA). The CT parameters were as follows: tube voltage of 120kVp, and slice thickness of 1,25 mm. Nonionic intravenous contrast material was injected before the CT scan. CT images were obtained before (non-enhanced) and after contrast administration at the portal venous phase.

Statistical analysis

Categorical variables were presented as frequency and percentage, and continuous variables were presented as mean and standard deviation (SD), and median and interquartile range (IQR). Continuous variables were checked for

conformity to normal distribution using graphical methods (P-P plot, Q-Q plot, and histogram) and statistical method (Shapiro-Wilk’s test). Hounsfield unit values of the lesions before and after contrast injection were compared using the Wilcoxon test. Taking the alpha level of 0.05, power of 80%, and Cohen’s medium-to-large effect size of 0.60, the minimum sample size was calculated as 25 people. A p-value of <0.05 was considered significant. Analyses were made using Stata v17 (Stata Corp, TX, USA).

Results

A total of 110 records were obtained. Two patients were excluded because of having non-contrast CT and 1 patient was excluded due to absence of preoperative CT (Figure 1). Therefore, 107 patients were included in the study. Of these, 60 (56%) were female and 47 (44%) were male and the mean age was 57.9 ± 14.8 years (median [IQR] age was 52.5 [59 – 68] years). Localizations of SELs are given in Table 1.

Table 1. Localizations of subepithelial lesions.

Localization	n (%)
Esophagus	7 (6.5)
Stomach	62 (57.9)
Duodenum	21 (19.6)
Jejunum	5 (4.6)
Ileum	2 (1.8)
Colon	9 (8.4)
Extramural	1 (0.9)

Characteristics of the lesions that were not detected on CT

In 22 (20.6%) patients, the lesion was not detected on CT. Among these 22 patients, 10 had only endoscopic examination without EUS (Figure 1). All of the lesions that could not be seen on CT were less than 2 cm in size. In two patients, the size of the lesions was not measured on

Table 2. Pre- and post-contrast Hounsfield Unit (HU) values.

		Before	After	p
GIST	Mean ± SD	34.4 ± 13.5	76.2 ± 35.7	0.003
	Median (IQR)	30 (29 – 38)	70 (57 – 77)	
NET	Mean ± SD	36.0 ± 5.5	104.5 ± 31.6	0.068
	Median (IQR)	36.5 (32 – 40)	101.5 (81.5 – 127.5)	
Leiomyoma	Mean ± SD	42.4 ± 7.5	57.7 ± 2.5	0.109
	Median (IQR)	43 (35 – 50)	58 (55 – 60)	
Schwannoma	Mean ± SD	22.5 ± 6.4	64.0 ± 22.6	0.178
	Median (IQR)	22.5 (18 – 27)	64 (48 – 80)	
Lipoma	Mean ± SD	-88.3 ± 35.2	-84.3 ± 39.8	0.285
	Median (IQR)	-78 (-128 – -60)	-66 (-130 – -57)	

GIST, gastrointestinal stromal tumors; IQR, interquartile range, NET neuroendocrine tumors; SD, standard deviation.

Table 3. Subepithelial lesions: pathological diagnoses.

Pathology	n (%)
GIST	13 (52)
NET	5 (20)
Leiomyoma	3 (12)
Schwannoma	2 (8)
Castleman Disease	1 (4)
Appendix Mucinous Neoplasm	1 (4)

GIST, gastrointestinal stromal tumors; NET neuroendocrine tumors.

endoscopy. In the remaining 8 patients, lesion size was between 5 and 20 mm (mean 11.5 ± 6.2 mm, and median [IQR] 10 [6-17.5] mm). In patients who underwent EUS, the size of the lesions ranged between 5 and 16 mm (mean 9.9 ± 4.3 mm; median [IQR] 10 [6-15] mm).

The lesions were not visualized with CT due to several reasons. In one patient, the lesion was located in the cardia and could not be visualized on CT due to the presence of motion artifacts and sliding hernia. In one patient, the lesion was described as indistinguishable for SEL or edema on colonoscopy, and that lesion was not observed on CT, which is probably a true negative result. Gastrointestinal distension was insufficient in the majority of patients in whom the lesion could not be visualized on CT.

HU values before and after contrast injection are shown in Figure 2 and Table 2. While the HU values increased by approximately 3 times in patients diagnosed with neuroendocrine tumors (NET) (median [IQR] values 36.5 [32 - 40] vs. 101.5 [81.5 - 127.5]; $p = 0.068$), the increase was approximately 2 times in those with gastrointestinal stromal tumors (GIST) (30 [29 - 38] vs. 70 [57 - 77]; $p=0.003$; Figure 2).

Pathological diagnosis, endoscopy, and CT findings

Pathology results were available in 25 (23.36%) patients, and the diagnoses of these patients are given in Table 3.

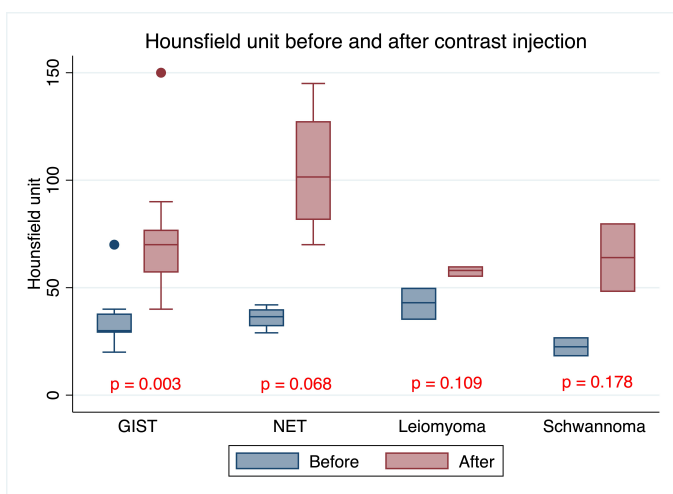


Figure 2. Hounsfield units before and after contrast injection in subepithelial lesions.

The lesions that did not have a pathologic diagnosis but were diagnosed with CT were 3 lipomas (Figure 3), 2 ec-



Figure 3. Coronal CT image of jejunal lipoma, which is shown with an asterisk in the center of the mass.

topic pancreas, and 3 extraintestinal organ compressions. In one patient with suspected SEL, there was an infected collection due to a gallbladder operation. In this case, CT diagnosis was based on the reactionary wall thickening in the prepyloric antrum of the stomach. In two patients with suspected SEL on endoscopy or EUS, calcifications were detected on CT, one in the stomach and the other one in the duodenum.

In 12 patients, there was an associated LAP, of which seven had a pathological diagnosis. The pathologic diagnoses of these cases were GIST (n=3) (Figure 4), NET (n=2) (Figure 5), hepatocellular carcinoma (HCC) and conglomerated lymphadenopathy (LAP) (n=1), and Castleman Disease (n=1).

Discussion

SEL of the gastrointestinal tract are lesions arising from the mucosa, submucosa, or muscularis propria and covered by the normal epithelium. Different lesions originate from different layers, so it is important to identify the origin. EUS is superior to CT in showing the wall layer from which the lesion originates. EUS also guides the therapeutic approach [12]. CT is superior over EUS in demonstrating lesion size, extent, and presence of invasion to surrounding organs or distant metastasis [10]. Also, CT can be used for staging of malignant lesions.

Differentiation of intramural or extramural (external compression) SELs can be made with high sensitivity with EUS [13]. Extramural compression may be caused by the spleen, splenic artery, pancreas, gallbladder, and left lobe of the liver. Pathological structures such as pseudocysts, vascular aneurysms, and tumors may also be the cause of



Figure 4. Axial CT image of gastrointestinal stromal tumor located in the jejunum. The border of the big lesion is marked with arrows. An air-fluid level is seen in the center of the mass.

compression [14, 15]. In a retrospective study comparing CT and EUS, 71 lesions measured less than 5 cm in diameter were evaluated and the accuracy rates of CT and EUS were close to each other (78.9% and 74.6%, respectively). However, there are studies reporting that lesions smaller than 10 mm in diameter cannot be detected on CT [11, 16]. In our study, all lesions that were not detected on CT were less than 20 mm in size.

The sensitivity and specificity of EUS in demonstrating the malignant potential of lesions have been found to be 64% and 80%, respectively [17]. The accuracy of fine needle aspiration biopsy (FNAB) in the diagnosis of SEL has been found between 46-93% [18, 19]. The wide range in accuracy rates may be due to that the lesion sizes differed substantially between the studies [20]. The diagnostic accuracy, sensitivity, and specificity of these methods were found to be higher in lesions larger than 2 cm in size [21, 22]. In the present study, only 5 of the patients (20%) with pathologically confirmed diagnoses were less than 2 cm in size. At the same time, some lesions are difficult to access with EUS, which may affect the diagnostic value of EUS.

In our study, pathological confirmation was obtained only in 25 (20%) patients. This is partly caused by no need for pathological confirmation in some patients such as lipoma, ectopic pancreas, or compression effect. Due to a low number of pathological confirmations, we did not assess the diagnostic performance of EUS or CT. Instead, we aimed to provide some diagnostic properties that may be help-

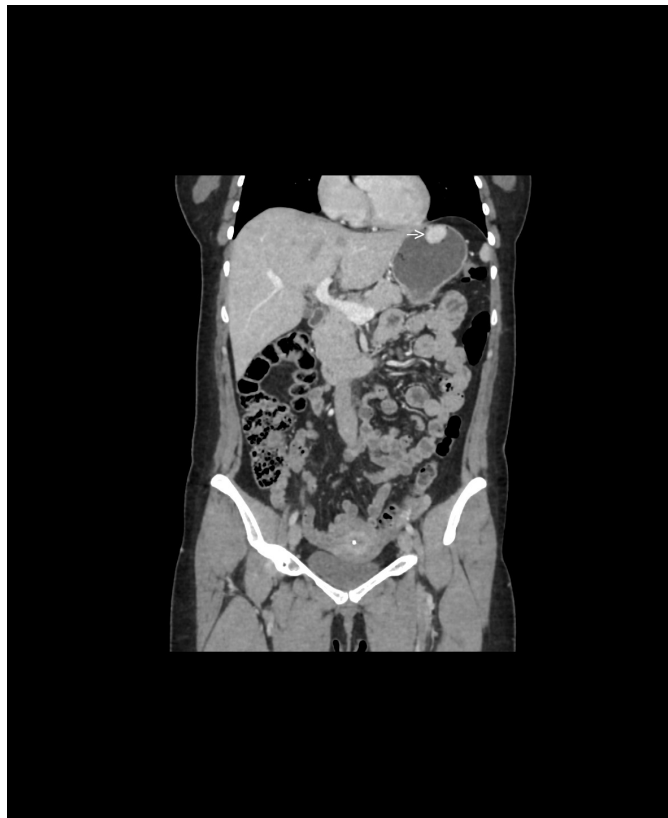


Figure 5. Coronal CT images of neuroendocrine tumor located in the gastric fundus, which is shown with arrow.

ful in differential diagnosis. Especially in lesions smaller than 1 cm, inadequate GI distension or inappropriate contrast phase may make CT diagnosis difficult. In addition, lesions located in the cardia may be difficult to visualize and attention should be paid to this region in the evaluation.

It may be more possible to differentiate GI wall layers in the arterial phase on CT. In addition, hypervascular tumors are better visualized in the arterial phase [23, 24]. Therefore dynamic CT scanning may be useful. However, routine single-phase acquisition is performed in portal phase. In addition, differences in the dose of contrast medium and the degree of GI distension may complicate the visualization of GI wall layers on CT [25]. Adequate luminal distension and correct adjustment of intravenous contrast agent dose and CT acquisition phase provide optimal image acquisition on CT. In some of the patients in our study in whom we could not detect the lesion on CT, GI luminal distension was insufficient. Therefore, the patient should be given water to ensure luminal distension before the examination.

CT may be useful in differentiating epithelial and subepithelial lesions. Epithelial lesions usually show asymmetric irregular wall thickening, mucosal ulceration, and heterogeneous contrast enhancement patterns. On the other hand, subepithelial lesions are usually well-circumscribed, have a smooth surface, and show intraluminal or extraluminal growth [26]. The ability to obtain multiplanar images with CT may provide a better understanding of the intramural or extramural origin of the lesion.

GIST should be considered in the differential diagnosis of hypervascular intramural lesions larger than 3 cm detected on CT [27]. Consistent with previous studies, gastrointestinal stromal tumors were the most common subepithelial lesions in our study (52% of patients with pathologically diagnosed cases). In the EUS reports of our patients, all GIST cases were reported to be originated from muscularis propria. GISTs are originated from interstitial Cajal cells and these cells are located in the muscularis propria [28]. Therefore, EUS reports stating that the lesion originates from the muscularis propria may bring the radiologist closer to the diagnosis of GIST.

Knowing the attenuation values of the lesions also contributes to the differential diagnosis. Previous studies have reported mean density values of 30-35 HU before contrast and 50-60 HU in post-contrast images for GIST on CT [8, 29]. In our study, HU increased by 2 times in patients with GIST ($p = 0.003$). Of note, in patients with NET, HU increased by 3 times with a borderline significance ($p = 0.068$). Despite a prominent increase in HU, the presence of borderline significance is probably caused by low power due to a low number of patients with NET ($n=4$). NETs show prominent contrast enhancement in the arterial phase. Consistent with the literature, 4 patients with NET in our series showed significant contrast enhancement after contrast injection [23, 24]. In one study, gastric GIST and non-GIST lesions were compared [30]. When the pre-contrast and post-contrast HU values of the lesions were compared, the mean HU values of GISTs were found to be lower than Non-GISTs (Leiomyoma and schwannoma).

The localization of the lesion may also be helpful for the diagnosis. Lesions located in the gastric cardia may be more likely to be leiomyoma, while those located in the corpus and fundus may be more likely to be GIST, and those located in the antrum may be more likely to be ectopic pancreas [31]. We had 3 patients with pathologically confirmed leiomyoma, and 2 of them were located in the cardia and one in the antrum. In one patient, the diagnosis of ectopic pancreas was confirmed and it was located in the antrum. The body of the stomach is the most common location of gastric GISTs, which is followed by fundus, antrum, and cardia [32, 33]. Consistently, in our study 5 (38.46%) GISTs were localized in the corpus, one in the antrum (7.69%), one in the fundus (7.69%), one in the duodenum (7.69%), 4 in the jejunum (30.7%), one in the ileum (7.69%). It should be noted that diagnosis of GISTs located in the cardia is difficult with EUS and might be confused with leiomyoma [31].

In a study comparing EUS and CT in gastric SEL cases, EUS was found to be more reliable in the diagnosis of leiomyoma and ectopic pancreas among benign pathologies, while CT was more valuable in the diagnosis of lipoma and gastric duplication cyst [32]. In our study, 3 patients were diagnosed with lipoma by CT without a need for pathological confirmation. Similarly, good results are obtained with CT in the detection of extraluminal compressive structures. We detected extraintestinal organ (spleen, diaphragm, pancreas) compression in 3 patients.

CT is less likely to predict histologic diagnosis than EUS. In a study of 53 patients, the overall accuracy of CT for histologic diagnosis was 50.9%. and EUS %64.2 [34].

Knowledge of the lesion characterization is of great importance for determining the treatment option. The size of the lesion, histopathology, and whether it has malignant potential or symptomatic are the factors that are taken into consideration in determining follow-up or treatment options [35].

This study has some limitations. First, it is a retrospective study and obtained from a single center. Second, the number of patients is relatively low. Third, the number of pathologically confirmed lesions is low, but it is mostly due to CT diagnoses that do not require confirmation. On the other hand, the CT findings were not based on the CT reports but were interpreted by an experienced radiologist for this study, which may be considered a strength of this study.

Conclusion

In conclusion, the present study provides CT characteristics of the SELs, and along with the endoscopy or EUS findings, it gives some properties (such as localization, CT attenuation values, and contrast enhancement) that might be useful in assessing SELs and their differential diagnosis. The conditions that the radiologist should pay attention to when evaluating this preliminary diagnosis are emphasized. Of note, in patients with a prediagnosis of SEL, providing adequate GI distension before the CT examination and performing the examination dynamically in three phases may increase the diagnostic value of CT.

Ethical approval

This study was approved by the institutional ethics committee (Ankara Bilkent City Hospital Medical Research Scientific and Ethical Evaluation Board No. 2 (TABED), 15 May 2024; 2-24-165).

References

- Hedenbro JL, Ekelund M, Wetterberg P. Endoscopic diagnosis of submucosal gastric lesions. The results after routine endoscopy. *Surg Endosc* 1991;5:20-23.
- Aghdassi A, Christoph A, Dombrowski F, et al. Gastrointestinal Stromal Tumors: Clinical Symptoms, Location, Metastasis Formation, and Associated Malignancies in a Single Center Retrospective Study. *Dig Dis* 2018; 36:337-345.
- Polkowski M. Endoscopic ultrasound and endoscopic ultrasound-guided fine-needle biopsy for the diagnosis of malignant submucosal tumors. *Endoscopy* 2005; 37:635-645.
- Hwang JH, Kimmey MB. The incidental upper gastrointestinal subepithelial mass. *Gastroenterology* 2004;126:301-307.
- Ponsaing LG, Kiss K, Loft A, et al. Diagnostic procedures for submucosal tumors in the gastrointestinal tract. *World J Gastroenterol* 2007; 13:3301-3310.
- Alkhatib AA, Faigel DO. Endoscopic ultrasonography-guided diagnosis of subepithelial tumors. *Gastrointest Endosc Clin N Am* 2012; 22:187-205.
- Brand B, Oesterhelweg L, Binmoeller K F, et al. Impact of endoscopic ultrasound for evaluation of submucosal lesions in gastrointestinal tract. *Dig Liver Dis* 2002; 34:290-297.
- Lee CM, Chen HC, Leung TK, Chen YY. Gastrointestinal stromal tumor: computed tomographic features. *World J Gastroenterol* 2004; 10:2417-2418.
- Megibow AJ, Balthazar EJ, Hulnick DH, et al. CT evaluation of gastrointestinal leiomyomas and leiomyosarcomas. *AJR Am J Roentgenol* 1985; 144:727-731.
- Ra JC, Lee ES, Lee JB, et al. Diagnostic performance of stomach CT compared with endoscopic ultrasonography in diagnosing gastric subepithelial tumors. *Abdom Radiol (NY)* 2017; 42:442-450.

11. Goto O, Kambe H, Niimi K, et al. Discrepancy in diagnosis of gastric submucosal tumor among esophagogastroduodenoscopy, CT and endoscopic ultrasonography: a retrospective analysis of 93 consecutive cases. *Abdom Imaging* 2012; 37:1074-1078.
12. Irisawa A, Yamao K. Curved linear array EUS technique in the pancreas and biliary tree: Focusing on the stations. *Gastrointest. Endosc.* 2009;69: 84-89.
13. Rösch T, Kapfer B, Will U, et al. Accuracy of endoscopic ultrasonography in upper gastrointestinal submucosal lesions: A prospective multicenter study. *Scand. J. Gastroenterol.* 2002;37: 856-862.
14. Motoo Y, Okai T, Ohta H, et al. Endoscopic ultrasonography in the diagnosis of extraluminal compressions mimicking gastric submucosal tumors. *Endoscopy* 1994; 26:239-242.
15. Hwang JH, Saunders MD, Rulyak SJ, et al. A prospective study comparing endoscopy and EUS in the evaluation of GI subepithelial masses. *Gastrointest. Endosc.* 2005; 62: 202-208.
16. Liu M, Liu L, Jin E. Gastric sub-epithelial tumors: Identification of gastrointestinal stromal tumors using CT with a practical scoring method. *Gastric Cancer* 2019; 22:769-777.
17. Cho JW. Current Guidelines in the Management of Upper Gastrointestinal Subepithelial Tumors. *Clin Endosc* 2016; 49:235-240.
18. Faulx AL, Kothari S, Acosta RD, et al. The role of endoscopy in subepithelial lesions of the GI tract. *Gastrointest Endosc* 2017; 85:1117-1132.
19. Pih GY, Kim DH. Endoscopic Ultrasound-Guided Fine Needle Aspiration and Biopsy in Gastrointestinal Subepithelial Tumors. *Clin Endosc* 2019; 52:314-320.
20. Wani S, Muthusamy VR, Komanduri S. EUS-guided tissue acquisition: an evidence-based approach (with videos). *Gastrointest Endosc* 2014; 80:939-959.
21. Akahoshi K, Oya M, Koga T, et al. Clinical usefulness of endoscopic ultrasound-guided fine needle aspiration for gastric subepithelial lesions smaller than 2 cm. *J. Gastrointest. Liver Dis. JGLD* 2014; 23:405-412.
22. De Moura DTH, McCarty TR, Jirapinyo P, et al. EUS-guided fine-needle biopsy sampling versus FNA in the diagnosis of subepithelial lesions: A large multicenter study. *Gastrointest. Endosc.* 2020;92: 108-119.
23. Sippel RS, Chen H. Carcinoid tumors. *Surg Oncol Clin N Am* 2006;15 :463-478.
24. Horton KM, Kamel I, Hofmann L, Fishman EK. Carcinoid tumors of the small bowel: a multitech-nique imaging approach. *AJR Am J Roentgenol* 2004; 182:559-567.
25. Mani NB, Suri S, Gupta S, Wig JD. Two-phase dynamic contrast-enhanced computed tomography with water-filling method for staging of gastric carcinoma. *Clin Imaging* 2001; 25:38-43.
26. Horton KM, Fishman EK. Current role of CT in imaging of the stomach. *RadioGraphics* 2003; 23:75-87.
27. Lee NK, Kim S, Kim GH, et al. Hypervascular Subepithelial Gastrointestinal Masses: CT-Pathologic Correlation. *RadioGraphics* 2010; 30:1915-34.
28. Ulsan S, Koc Z, Kayaselcuk F. Gastrointestinal stromal tumours: CT findings. *Br J Radiol* 2008; 81:618-623.
29. Ludwig DJ, Traverso LW. Gut stromal tumors and their clinical behavior. *Am J Surg* 1997; 173:390-394.
30. Liu M, Liu L, Jin E. Gastric sub-epithelial tumors: identification of gastrointestinal stromal tumors using CT with a practical scoring method. *Gastric Cancer* 2019; 22:769-777.
31. Kim SY, Shim KN, Lee JH, et al. Comparison of the Diagnostic Ability of Endoscopic Ultrasonography and Abdominopelvic Computed Tomography in the Diagnosis of Gastric Subepithelial Tumors. *Clin Endosc.* 2019; 52:565-573.
32. Min YW, Park HN, Min BH, et al. Preoperative predictive factors for gastrointestinal stromal tumors: Analysis of 375 surgically resected gastric subepithelial tumors. *J Gastroenterol Surg* 2015;19: 631-638.
33. Seo SW, Hong SJ, Han JP, et al: Accuracy of a scoring system for the differential diagnosis of common gastric subepithelial tumors based on endoscopic ultrasonography. *J Digest Dis* 2013; 14: 647-653.
34. Goto O, Kaise M, Lwakiri K. Advancements in the Diagnosis of Gastric Subepithelial Tumors. *Gut Liver.*2022; 16:321-330.
35. Sharzehi K, Sethi A, Savides. AGA Clinical Practice Update on Management of Subepithelial Lesions Encountered During Routine Endoscopy: Expert Review. *Clin Gastroenterol Hepatol.*2022; 20:2435-2443.